Stromal Cell–Derived Factor-1 Promotes Cell Migration and Tumor Growth of Colorectal Metastasis[1]

Otto Kollmar, Kathrin Rupertus*, Claudia Scheuer†, Bastian Junker*, Bettina Tilton*, Martin K. Schilling* and Michael D. Menger†*

*Department of General, Visceral, Vascular, and Pediatric Surgery, University of Saarland, D-66421 Homburg/Saar, Germany; †Institute for Clinical and Experimental Surgery, University of Saarland, D-66421 Homburg/Saar, Germany

Abstract

In a mouse model of established extrahepatic colorectal metastasis, we analyzed whether stromal cell–derived factor (SDF) 1 stimulates tumor cell migration *in vitro* and angiogenesis and tumor growth *in vivo*. *METHODS:* Using chemotaxis chambers, CT26.WT colorectal tumor cell migration was studied under stimulation with different concentrations of SDF-1. To evaluate angiogenesis and tumor growth *in vivo*, green fluorescent protein–transfected CT26.WT cells were implanted in dorsal skinfold chambers of syngeneic BALB/c mice. After 5 days, tumors were locally exposed to SDF-1. Cell proliferation, tumor microvascularization, and growth were studied during a further 9-day period using intravital fluorescence microscopy, histology, and immunohistochemistry. Tumors exposed to PBS only served as controls. *RESULTS: In vitro*, > 30% of unstimulated CT26.WT cells showed expression of the SDF-1 receptor CXCR4. On chemotaxis assay, SDF-1 provoked a dose-dependent increase in cell migration. *In vivo*, SDF-1 accelerated neovascularization and induced a significant increase in tumor growth. Capillaries of SDF-1–treated tumors showed significant dilation. Of interest, SDF-1 treatment was associated with a significantly increased expression of proliferating cell nuclear antigen and a downregulation of cleaved caspase-3. *CONCLUSION:* Our study indicates that the CXC chemokine SDF-1 promotes tumor cell migration *in vitro* and tumor growth of established extrahepatic metastasis *in vivo* due to angiogenesis-dependent induction of tumor cell proliferation and inhibition of apoptotic cell death.

Neoplasia (2007) **9,** 862–870

Keywords: Cancer, metastasis, chemokine, SDF-1, angiogenesis.

Introduction

Colorectal cancer is one of the leading causes of cancer-related deaths among men and women worldwide. Death usually results from uncontrolled metastatic disease. The liver is the most common site of metastasis, and surgical resection is the only option for curative treatment, reflected by a 5-year overall survival rate of up to 58% [1–4]. In contrast, manifestation of extrahepatic metastases has long been considered as a contraindication to resection of hepatic lesions. Some recent studies, however, showed promising 5-year survival rates of ~ 30% after sequential resection of hepatic and extrahepatic colorectal metastases [5–7].

The metastatic process consists of a series of individual steps, which all are required to establish metastatic tumors [8,9]. Whereas chemokines and their receptors are known to be involved in the "homing" of hematopoietic cells to specific organs as a physiological mechanism [10], homing is also functional in neoplastic cells [11]. Recent studies have shown that tumor cells express patterns of chemokine receptors and that corresponding ligands are specifically expressed in organs to which these cancers commonly metastasize. For example, breast cancer cells and primary breast cancers have been shown to express the chemokine receptor CXCR4, whereas the specific ligand CXCL12, also known as stromal cell–derived factor (SDF) 1, has been found at elevated levels in lymph nodes, lung, liver, and bone marrow—organs that represent the first metastatic sites of breast cancer [12]. Others also speculated on the involvement of CXCR4 in the metastatic tumor growth of different types of malignancies, including colorectal cancer [13–15]. As shown by Ottaiano et al. [15], the lack of CXCR4 and vascular endothelial growth factor (VEGF) expression in both primary tumors and metastases is a strong prognostic factor for the disease-free survival of colorectal cancer patients [16].

Although several studies have indicated that the CXCR4 receptor may be involved in the metastatic process of colorectal cancer, the functional role of SDF-1 has not been identified yet. With the use of a murine colon cancer model, we therefore studied whether SDF-1 affects the process of

Address all correspondence to: Otto Kollmar, MD, Department of General, Visceral, Vascular, and Pediatric Surgery, University of Saarland, D-66421 Homburg/Saar, Germany.
E-mail: otto.kollmar@uniklinikum-saarland.de

[1]This study was supported by grants from the Research Committee and the Medical Faculty of the University of Saarland (HOMFOR-A/2003/1).
Received 5 July 2007; Revised 15 August 2007; Accepted 20 August 2007.

DOI 10.1593/neo.07559

angiogenesis and the tumor growth of established extrahepatic metastasis *in vivo*.

Materials and Methods

Tumor Cell Lines and Culture Conditions

The CT26 cell line is a *N*-nitroso-*N*-methylurethane–induced undifferentiated adenocarcinoma of the colon, syngeneic with BALB/c mice. For our studies, the CT26.WT cell line (ATCC CRL-2638; LGC Promochem GmbH, Wesel, Germany) was grown in cell culture as a monolayer in RPMI 1640 medium with 2 mM L-glutamine (Sigma Aldrich Chemie GmbH, Taufkirchen, Germany) supplemented with 10% fetal calf serum (FCS Gold; PAA Laboratories GmbH, Cölbe, Germany), 100 U/ml penicillin, and 100 μg/ml streptomycin (PAA Laboratories GmbH). The cells were incubated at 37°C in a humidified atmosphere containing 5% CO_2. With the use of CLONfectin (Clontech, Palo Alto, CA), CT26.WT cells were transfected with the enhanced green fluorescent protein (GFP) expression vector pEGFP-N1 (Clontech), in accordance with the manufacturer's instructions [17]. GFP transfection was performed by cloning. For individual *in vitro* and *in vivo* experiments, only cells of the first three serial passages after cryostorage were used. On the day of implantation, CT26.WT-GFP cells were harvested from subconfluent cultures (70–85%) by trypsinization (0.05% trypsin and 0.02% EDTA; PAA Laboratories GmbH) and washed twice in phosphate-buffered saline (PBS) solution.

Flow Cytometric Analysis of CT26.WT Cells

FACScan (Becton Dickinson, Mountain View, CA) analysis was performed to assess the expression of the chemokine receptor CXCR4 on CT26.WT and CT26.WT-GFP cells in triplicate. After trypsinization, the cells were fixed in 1 ml of Cytofix/Cytoperm (BD Biosciences, Heidelberg, Germany) for 20 minutes at 4°C, washed twice with Perm Wash (BD Biosciences), and incubated at room temperature for 40 minutes with a polyclonal goat anti-mouse CXCR4 antibody (Santa Cruz, Heidelberg, Germany) or an isotype-matched control antibody (Dianova, Hamburg, Germany). A rabbit anti-goat Cy3-conjugated antibody (1:25; Dianova) was used for fluorescence labeling. To remove excess antibody, cells were washed again and then maintained in 1% paraformaldehyde in PBS. A flow cytometer was calibrated with fluorescent standard microbeads (CaliBRITE Beads; BD Biosciences) for accurate instrument setting. Tumor cells were selectively analyzed for their fluorescence properties using the CellQuest data handling program (BD Biosciences), with assessment of 5000 events per sample.

Cell Migration Assay

The migration capability of CT26.WT cells was assessed using 24-well chemotaxis chambers and polyvinylpyrrolidone-coated polycarbonate filters with an 8-μm pore size (BD Falcon, Heidelberg, Germany). Chemotaxis assays were performed in triplicate. The chemoattractant SDF-1 (recombinant mouse SDF-1α/CXCL12, no. 460-SD; R&D Systems, Wiesbaden, Germany), diluted in PBS with 0.1% BSA (Sigma Aldrich Chemie GmbH), was added in concentrations of 0.1, 1, 10, 100, 200, and 400 nM to 700 μl of RPMI 1640 medium in lower wells. PBS with 0.1% BSA alone served as control. Five hundred microliters of a cell suspension containing 1×10^5 cells in RPMI 1640 was added to each of the upper wells. Then the chamber was incubated for 24 hours at 37°C in a humidified atmosphere with 5% CO_2. After incubation, nonmigrated cells were removed from the upper surface of the filters, and migrated cells, which are adherent to the lower surface, were fixed with methanol and stained with Dade Diff-Quick (Dade Diagnostika GmbH, München, Germany). The number of these migrated cells was counted in 10 high-power microscopic fields. In addition, the cells that had migrated into the lower wells were collected and counted by FACScan flow cytometry. Migrated cells that are adherent to the lower surface of the filters are expressed as the number of cells per 10 high-power fields; cells that had migrated to the lower wells are expressed as the number of cells per well.

Animals

Experiments were performed after approval by the local governmental ethics committee and conformed to the United Kingdom Coordinating Committee on Cancer Research Guidelines for the Welfare of Animals in Experimental Neoplasia (as described in 1998 in *Br J Cancer* **77**, 1–10) and the Guide for the Care and Use of Laboratory Animals (Institute of Laboratory Animal Resources, National Research Council; NIH Guide, Vol. 25, No. 28, 1996). Twelve- to 16-week-old female BALB/c mice (Charles River Laboratories GmbH, Sulzfeld, Germany) with a body weight of 18 to 22 g were used. The animals were housed in single cages at room temperature (22–24°C) and at relative humidity (60–65%) with a 12-hour light/dark cycle environment. The mice were allowed free access to drinking water and standard laboratory chow (Altromin, Lage, Germany).

Experimental Model

For operative procedures, animals were anesthetized with an intraperitoneal injection of 90 mg/kg body weight ketamine (Ketavet; Parke Davis, Freiburg, Germany) and 20 mg/kg body weight xylazine (Rompun; Bayer, Leverkusen, Germany). To allow repetitive analyses of the microcirculation of growing tumors, the dorsal skinfold chamber model was used for intravital microscopy, as previously described in detail [18]. The chamber consists of two symmetrical titanium frames (weight, 3.2 g), which were positioned to sandwich the extended double layer of the dorsal skin. One layer was completely removed in a circular area 15 mm in diameter. The remaining layers, consisting of the epidermis, subcutaneous tissue, and striated skin muscle, were covered with a glass coverslip incorporated into one of the titanium frames [19]. The animals tolerated the chambers well and showed no signs of discomfort or changes in sleeping and feeding habits. After a 48-hour recovery period, the coverslip of the chamber was temporarily removed, and 1×10^5 cells were implanted onto

the surface of the striated muscle tissue within the chamber. Directly after cell implantation, the chamber tissue was covered again with the coverslip [20].

Experimental Protocol

Sixteen animals received tumor cell implantation. After 5 days (day 0), the animals were assigned to two different groups. The dorsal skinfold chamber was opened, and SDF-1 was locally applied (SDF-1; $n = 8$). The concentration was 100 nM in the final preparation. This concentration was directly exposed to the tissue within the dorsal skinfold chamber. Accordingly, this was also the concentration in the skinfold chamber at the time of treatment. Animals that received only PBS served as controls (Control; $n = 8$). All animals underwent repetitive intravital microscopic analyses directly before—as well as 2, 4, 7, and 9 days after—SDF-1 exposure. At the end of the experiment, the chamber with the tumor tissue was harvested for histology and immunohistochemistry.

Intravital Fluorescence Microscopy

Intravital fluorescence microscopy was performed with epi-illumination technique using a modified Zeiss Axio-Tech microscope (Zeiss, Oberkochen, Germany) with a 100-W HBO mercury lamp. Microscopic images were monitored by a charge-coupled device video camera (FK 6990, COHU; Prospective Measurements, Inc., San Diego, CA) and were transferred to a video system (VO-5800 PS; Sony, München, Germany) for subsequent off-line analysis. Tumor size, growth kinetics, and neovascularization were analyzed using blue light epi-illumination (excitation wavelength, 450–490 nm; emission wavelength, > 520 nm) [21].

Microcirculation Analysis

Microcirculatory parameters were assessed off-line by a frame-to-frame analysis of videotaped images using a computer-assisted image analysis system (CapImage; Zeintl Software, Heidelberg, Germany). Data analysis was performed by examiners blinded to the treatment.

The fluorescent labeling of tumor cells allowed precise delineation of the tumor from the surrounding unaffected host tissue. At each observation time point, the surface of the fluorescently labeled tumor mass within the chamber was first scanned for determination of tumor size (expressed as tumor area in square millimeters). Next, eight regions of interest (ROI) were randomly chosen within the tumor margin. In these ROI, the onset of neovascularization (i.e., development of angiogenic buds, sprouts, and blood vessels) was documented and scored from 0 to 8, where 0 = *neovascularization in none of the ROI* and 8 = *neovascularization in all of the ROI* [22]. The functional capillary density (cm/cm^2) of the tumor microvasculature, defined as the length of red blood cell–perfused capillaries per observation area [23], was analyzed within the eight ROI of the tumor margin and within four additional ROI of the tumor center. Diameters of the newly formed tumor microvessels were measured perpendicularly to the vessel path and are expressed in micrometers [17].

Histology and Immunohistochemistry

At the end of the experiments (day 9), the tumor and adjacent host tissue were harvested. For light microscopy, formalin-fixed biopsies were embedded in paraffin. Five-micrometer sections were cut and stained with hematoxylin–eosin for routine histology, in accordance with standard procedures. Tumor cell invasion of the muscular layer was measured and expressed as a percentage of the length of the tumor basis [24].

To study cell proliferation and apoptotic cell death, proliferating cell nuclear antigen (PCNA) and cleaved caspase-3 were stained using indirect immunoperoxidase techniques. Therefore, deparaffinized sections were incubated with 3% H_2O_2 and 2% goat normal serum to block endogenous peroxidases and unspecific binding sites. A monoclonal mouse anti-pan PCNA antibody (PC10, 1:50; DakoCytomation, Hamburg, Germany) and a polyclonal rabbit anti-mouse cleaved caspase-3 antibody (Asp175, 1:50; Cell Signaling Technology, Frankfurt, Germany) were used as primary antibodies [25]. The cleaved caspase-3 antibody detects endogenous levels only of the short fragment (17/19 kDa) of activated caspase-3, but not full-length caspase-3. Biotinylated goat anti-mouse and goat–rabbit Ig antibodies were used as secondary antibodies for streptavidin–biotin complex peroxidase staining (1:200, LSAB 2 System HRP; DakoCytomation). 3,3′-Diaminobenzidine (DakoCytomation) was used as chromogen. Sections were counterstained with Mayer hemalum stain and examined by light microscopy.

To assess the expression of the chemokine receptor CXCR4, tumor slices were embedded in Tissue Freezing Medium (Jung; Leica Microsystems, Nussloch, Germany) for immunohistochemistry, snap-frozen in liquid nitrogen, and stored at −80°C. Five-micrometer cryostat sections were cut, fixed in 4°C cold acetone for 5 seconds and in 4% formalin for 10 minutes, and blocked with 2% normal donkey serum. Then tissue sections were incubated with a polyclonal goat anti-mouse CXCR4 antibody (1:10; Santa Cruz). A donkey anti-goat IgG HRP-conjugated antibody (1:500; Amersham, Freiburg, Germany) was used as secondary antibody. 3,3′-Diaminobenzidine was used as chromogen. Sections were counterstained with Mayer hemalum stain and examined by light microscopy.

As a negative control, additional slices from each specimen were exposed to appropriate IgG isotype–matched antibody (Sigma Aldrich Chemie GmbH), instead of the primary antibody, under the same conditions to determine the specificity of antibody binding. All of the control stainings were found to be negative.

Statistical Analysis

All values are expressed as mean ± SEM. After proving the assumption of normality and homogeneity of variance across groups, the groups studied were compared by a nested design, including analysis of variance and *post hoc* comparison with correction of α error according to Bonferroni probabilities to compensate for multiple comparisons. Statistical significance was set at $P < .05$. Statistical analyses were performed using the software package SigmaStat (SPSS, Inc., Chicago, IL).

Results

In Vitro *FACScan Analysis and Migration Assay*

FACScan analysis demonstrated that 31.5 ± 2.5% of CT26.WT cells were CXCR4 receptor–positive (Figure 1*A*). After transfection with the enhanced GFP expression vector pEGFP-N1, CT26.WT-GFP cells showed a comparable expression of CXCR4 (32.2 ± 4.3%) (Figure 1*B*). In cell culture, both cell lines had similar growth characteristics during the 7-day observation period (Figure 1*C*).

Migration assay indicated that only a few cells migrated under control conditions (i.e., with PBS stimulation; Figure 2). SDF-1 at a dose of 0.1 nM induced a 3.4-fold increase in cell migration at polycarbonate filters. With 1 nM SDF-1, this migration was most pronounced, as indicated by a 4.3-fold increase compared to controls (Figure 2*A*). Notably, a further increase in SDF-1 concentration resulted in a markedly decreased number of cells that were found to be adherent to the lower surface of the filters of the migration chambers. Analysis of the number of cells that had migrated through the filter to the lower wells indicated a 2-fold to 6-fold increase after low-dose SDF-1 stimulation (0.1–100 nM), whereas higher doses of 200 and 400 nM resulted in an exponential increase (16-fold to 17-fold) when compared with PBS controls (Figure 2*B*).

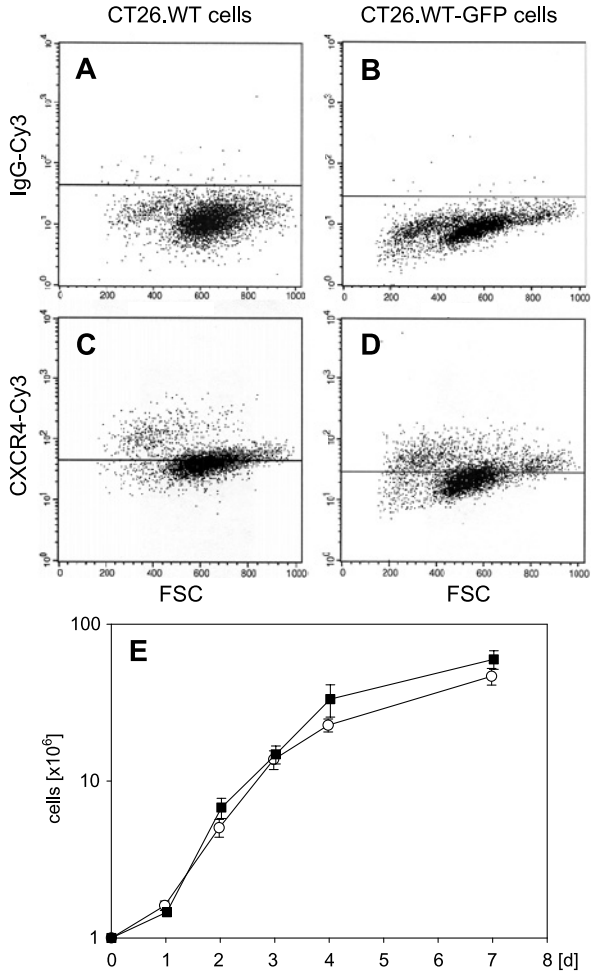

Figure 1. *FACScan analysis of CT26.WT (A and C; white squares) and CT26.WT-GFP (B and D; black squares) cells demonstrating ~ 30% positively stained cells for the chemokine receptor CXCR4 (C and D). Isotype-matched control antibody served as a negative control (A and B). Note that there is no difference in CXCR4 expression between GFP-transfected and nontransfected cells. The two cell lines showed comparable growth characteristics during the 7-day observation period (E). Data are expressed as mean ± SEM.*

Tumor Growth

The general conditions of all BALB/c mice were not affected by the implantation of the dorsal skinfold chamber and tumor cell implantation. All animals had an uneventful postoperative recovery, and they tolerated well intravital fluorescence microscopic observations during the 14-day period. The take rate of colorectal CT26.WT-GFP cells in the dorsal skinfold chamber was 100%. Intravital fluorescence microscopy showed progressive tumor growth during the entire observation period in both groups (Figure 3, *A* and *B*). Local application of SDF-1 on day 0 provoked a significant acceleration of tumor growth when compared with that measured in PBS controls. This was indicated by an increased tumor area at late time points during the 9 days of observation (Figure 3*C*).

Neovascularization

In both groups, analysis revealed a 40% to 50% neovascularization of the ROI of newly developed microvessels within the margin of the tumors on day 2. Of interest, on day 4, this ratio amounted to ~ 65% in controls, but was found to increase to > 95% after SDF-1 treatment (Figure 4*C*). At the end of the experiments, all ROI of both groups demonstrated new vessel formation within the tumor margin.

The vascular networks of the tumors were characterized by newly developed, chaotically arranged capillaries. The capillary density of these networks did not differ between tumor margin and tumor center (data not shown). Of interest, however, SDF-1–treated tumors had developed a higher density of newly formed tumor vessels within the tumor margin 4 days after SDF-1 application when compared to sham controls (Figure 4*D*). At the end of the experiment, the tumors of both groups showed a similar capillary density within their margins and centers.

Because neovascularization is regularly associated with vasodilation due to the action of VEGF, we analyzed capillary diameters within tumor vascular networks. Directly after SDF-1 treatment, newly formed capillaries at the tumor center showed significant ($P < .05$) dilation when compared with that of controls on days 2 and 4 (Figure 5). Capillary diameters of the tumor margins (data not shown) showed the same characteristics when compared to that observed in tumor centers.

Morphology, Proliferation, Apoptotic Cell Death, and CXCR4 Expression

Hematoxylin–eosin staining of the tumors on day 9 after SDF-1 exposure revealed solid extrahepatic growth within the dorsal skinfold chamber. In parallel to the significantly increased growth of the tumors after SDF-1 application,

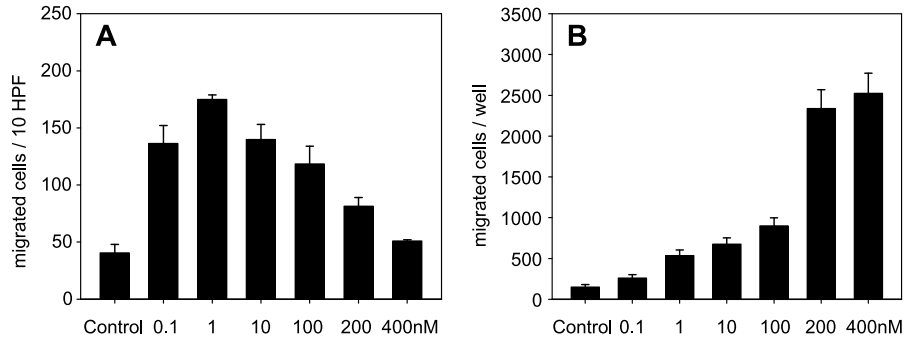

Figure 2. *Cell migration assay consisting of a chemotaxis chamber and polyvinylpyrrolidone-coated polycarbonate filters with an 8-μm pore size. Note that only a few cells migrate under control conditions (control in A and B), whereas stimulation with a low dose (1 nM) of SDF-1 exerts the most pronounced increase in the fraction of migrated cells adhering to the lower surface of the filters (A). In contrast, analysis of cell migration to the lower wells (B) shows a dose-dependent increase after SDF-1 exposure. Data are expressed as mean ± SEM.*

demonstrated by an increased tumor area during the 9 days of observation, quantitative analysis of histologic specimens showed a more invasive tumor growth with muscle infiltration after SDF-1 treatment. This was indicated by the infiltration of 23.3 ± 9.5% of the tumor basis after SDF-1 exposure when compared to 10.5 ± 6.3% in sham controls.

PCNA as an indicator of cell proliferation showed that almost 40% of the tumor cells displayed positive staining in controls (Figure 6, *A* and *E*). Notably, the rate of PCNA-positive cells was found to have significantly increased to > 70% after SDF-1 treatment (Figure 6, *B* and *E*). This indicates an increase in tumor cell proliferation directly mediated by SDF-1.

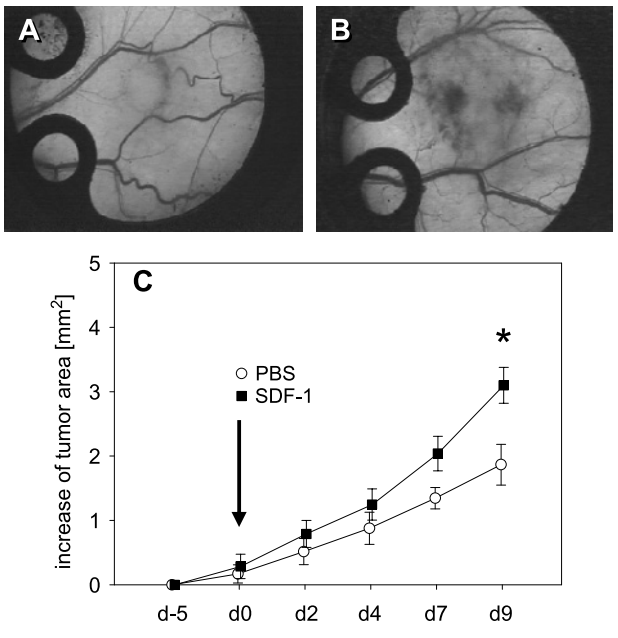

Figure 3. *Time course of tumor growth in dorsal skinfold chambers after implantation of CT26.WT-GFP cells in BALB/c mice. Day 9 stereomicroscopy photomicrographs of representative tumors from mice that underwent, on day 0, local sham treatment (A) and exposure to 100 nM SDF-1 (B). Quantitative analysis of the tumor area over time (C) shows progressive tumor growth in both sham-treated controls (white circles) and animals that underwent SDF-1 treatment (black squares). Note, however, that tumor growth after SDF-1 application is significantly increased compared to PBS controls. Data are expressed as mean ± SEM. *P < .05 vs PBS control. (A and B) Original magnification, ×4.*

To study apoptotic cell death, cleaved caspase-3 products were detected by immunohistochemistry. On day 9, a minor fraction of positively stained cells could be observed within the tumors (Figure 6, *C* and *D*). Of interest, quantitative analysis demonstrated a significantly ($P < .05$) lower fraction of apoptotic cells after SDF-1 application when compared with that of sham controls (Figure 6*F*).

Discussion

The major findings of the present study are that SDF-1 promotes a dose-dependent migration of colorectal cancer cells *in vitro* and tumor growth of solid metastasis *in vivo*. Of interest, the *in vivo* stimulation of growth is most probably induced by an angiogenesis-dependent induction of tumor cell proliferation and inhibition of apoptotic cell death.

Whereas many chemokines bind to more than one receptor, and chemokine receptors generally bind more than one chemokine, SDF-1 is still the only known ligand of CXCR4 [10,12]. In contrast, SDF-1 may bind not only to CXCR4 but also to CXCR7 [26]. SDF-1 induces the internalization of CXCR4-promoting calcium mobilization and activation of mitogen-activated protein kinase pathways, such as ERK-1/2, phosphatidylinositol 3-kinase (PI 3-kinase), and protein kinase B—kinases that have been implicated in cell migration, proliferation, differentiation, and survival [27].

CXCR4 is thought to facilitate the interaction between tumor cells and endothelial cells by activating rolling, integrin function, arrest, and transendothelial migration of tumor cells [28,29]. Although never proven *in vivo*, SDF-1 has been thought to direct the intratissue localization of tumor cells and to induce metastasis through direct effects on tumor cell migration [30,31], as recently suggested for the monocyte chemoattractant protein-1 CCL2 [32]. Using a non–small cell lung cancer cell line *in vitro*, Phillips et al. [33] have demonstrated a directional movement in response to a CXCL12–CXCR4 chemotactic gradient, with the highest amounts of migrated cells at a concentration of 10 ng/ml SDF-1. In line with others [34–36], our *in vitro* assay also showed a dose-dependent increase in tumor cell migration in response to SDF-1. This further supports an involvement of SDF-1 in metastatic tumor growth.

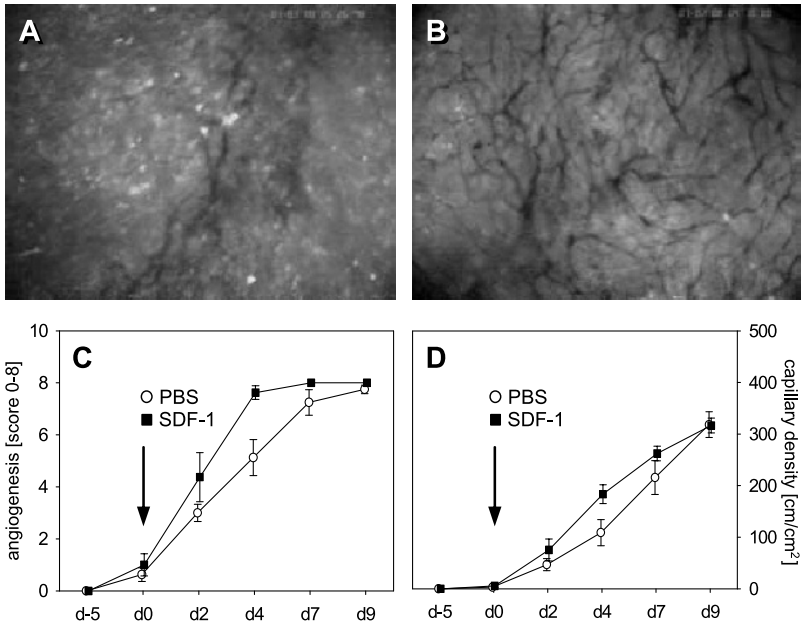

Figure 4. *Time course of neovascularization and functional capillary density of CT26.WT-GFP tumors in dorsal skinfold chambers as determined by intravital fluorescence microscopy. Fluorescence microscopic images display the capillary network in the tumor margins of a control animal (A) and an SDF-1–treated animal (B) on day 4. Analysis of the onset of neovascularization, expressed as a score from 0 to 8, (C) in control tumors (white circles) and SDF-1–treated tumors (black squares) showed accelerated angiogenesis after SDF-1 treatment compared to PBS controls (C). Analysis of capillary density within the tumor margin confirms an acceleration of vascularization due to SDF-1 treatment, as indicated by an increased capillary density on day 4 after chemokine exposure (D). Data are expressed as mean ± SEM. *P < .05* vs *PBS control. (A and B) Original magnification, ×40.*

A considerable number of previous studies have demonstrated that an overexpression of CXCR4 on tumor cells is associated with an increased tumor growth and a cancerous phenotype [28,36–38], and that neutralization of CXCR4 suppresses growth *in vivo* [13,14]. These data indicate a role for CXCR4 in tumor growth and metastasis; however, they did not prove the function of SDF-1. In fact, there is only sparse information on SDF-1 function in carcinogenesis *in vivo*. Orimo et al. [39] have demonstrated the inhibition of growth breast cancer cells *in vivo* by blockade of SDF-1. In contrast, Phillips et al. [33] have failed to demonstrate that neutralization of SDF-1 affects the size of primary non–small cell lung cancer tumors at orthotopic or heterotopic sites. Beside this controversy, there is no information on how direct SDF-1 exposure influences tumor growth *in vivo*. The results of the present study now demonstrate for the first time that SDF-1 application is capable of directly increasing tumor growth *in vivo*.

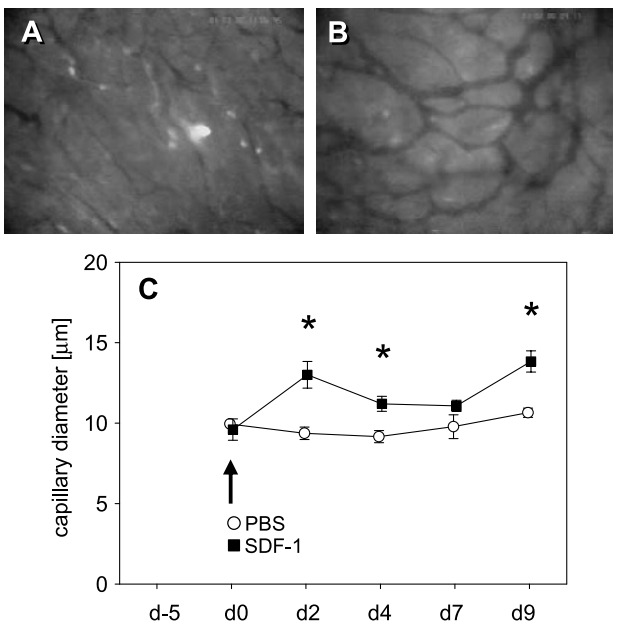

Figure 5. *Time course of capillary diameters of newly formed tumor vessels as determined by intravital fluorescence microscopy. Fluorescence microscopic images display the capillary network in the tumor center of a PBS control animal (A) and an SDF-1–treated animal (B) on day 9 after treatment induction. Quantitative analysis showed a significantly greater capillary diameter after SDF-1 exposure (black squares) when compared to PBS controls (white circles) (C). Data are expressed as mean ± SEM. *P < .05* vs *PBS control. (A and B) Original magnification, ×80.*

The mechanisms on how SDF-1 stimulates the outgrowth of established tumors and metastasis are not fully understood yet. There is some evidence that the chemokine influences both cell proliferation and apoptotic cell death. In a previous study, we have demonstrated that SDF-1 stimulation provokes nuclear translocation of both ERK-2, an accepted activator of transcription, and protein kinase B [27]. Others have further shown that SDF-1 induces mitogen-activated protein kinases and Akt activation, however, without influencing Fas ligand–induced apoptosis [35]. The SDF-1/CXCR4 pathway influences the growth of invasive and micrometastatic tumor cells [14], reflecting downstream signaling through the antiapoptotic AKT kinase [40] and the lipid kinase PI 3-kinase [41]. Several lines of evidence suggest that PI 3-kinase–mediated activation of protein kinase B inhibits apoptosis and promotes cell survival [42–44]. Furthermore, ERK-1/2 and Akt activation mediate antiapoptotic pathways and increase cell proliferation [40,42]. Although all

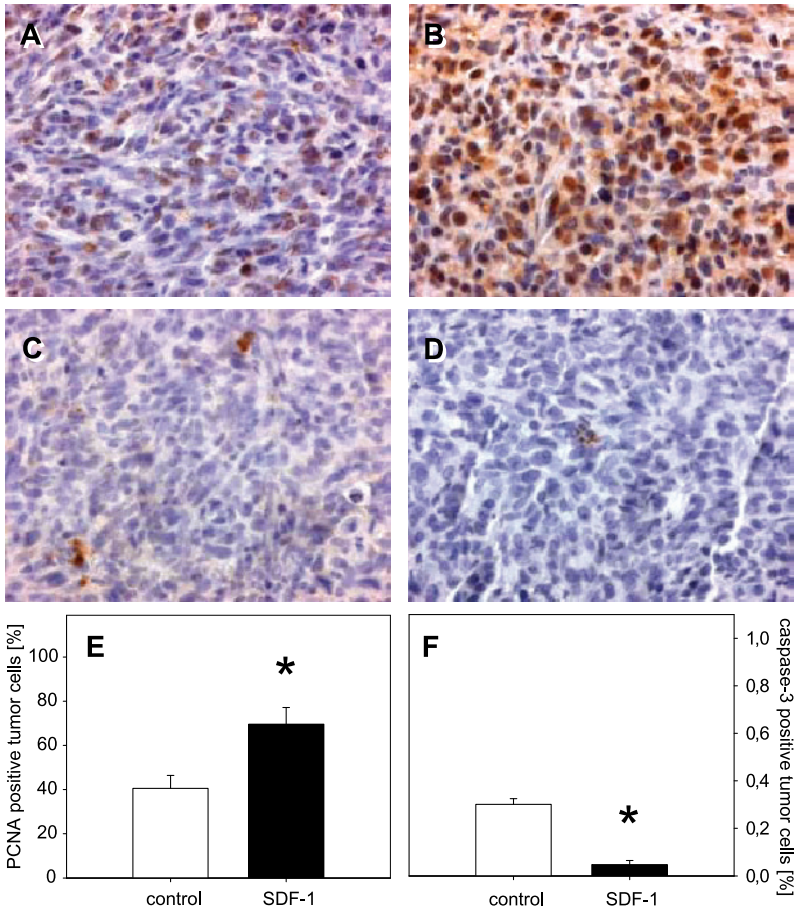

Figure 6. *PCNA (A and B) and cleaved caspase-3 (C and D) immunohistochemistry in CT26.WT-GFP tumors on day 9 after PBS (control; A and C) and SDF-1 treatment (SDF-1; B and D). Quantitative analysis of the number of PCNA-positive cells (expressed as a percentage of all cells) revealed significantly more positively stained cells in SDF-1–treated tumors when compared with tumors of controls (E). Analysis of cleaved caspase-3 expression (expressed as a percentage of all cells) showed a significantly reduced number of apoptotic cells after SDF-1 treatment when compared to PBS controls (F). Data are expressed as mean ± SEM. *P < .05 vs PBS control. (A–D) Original magnification, ×175.*

studies on the role of the SDF-1/CXCR4 pathway in cell proliferation and apoptotic cell death have been performed in *in vitro* setups [35,36], we herein demonstrate for the first time that SDF-1 is capable of stimulating tumor cell proliferation and of inhibiting apoptotic cell death also *in vivo*, and that these are most probably the cause of the observed chemokine-mediated stimulation of tumor growth.

Neoangiogenesis in tumors is determined by an imbalance in the overexpression of the proangiogenic factors and inhibiting factors of angiogenesis. CXC chemokines with a highly conserved three-amino-acid motif (Glu–Leu–Arg; ELR motif; ELR^+), including CXCL1–3 and CXCL5–8 (e.g., MIP-2 and IL-8), are potent promoters, whereas CXC chemokines lacking the ELR motif (ELR^-), including CXCL4, are potent inhibitors of angiogenesis [45]. Although SDF-1 is not an ELR^+ CXC chemokine, it is supposed to be involved in mediating angiogenesis by interacting with its receptor CXCR4 [46,47]. The SDF-1/CXCR4 pathway has been shown to be essential for development because mice deficient for CXCR4 or its ligand SDF-1 die perinatally due to major defects of the vascular system [48].

Using prostate tumors, Darash-Yahana et al. [28] have demonstrated a 4.5-fold increase in the number of blood vessels in tumors overexpressing CXCR4 and concluded that a high expression of this chemokine receptor accelerates angiogenesis by increasing the secretion of VEGF. These results are supported by the fact that neutralization of CXCR4 successfully inhibits the formation of new blood vessels [13,28]. *In vitro* studies have further shown that CXCR4 mediates tumor cell migration toward SDF-1 and that this migration is dependent on autocrine VEGF expression [46]. Of interest, SDF-1 may influence the expression of VEGF. Brand et al. [35] have demonstrated in the colorectal cancer cell line HT-29 that SDF-1 stimulation induces an 8-fold upregulation of VEGF mRNA expression and a 5.8-fold increase in VEGF protein levels.

These findings have been confirmed by Yang et al. [49] in glioblastoma cell lines, demonstrating that the expression of functional CXCR4 correlates with malignant phenotype and that stimulation with SDF-1 contributes to the production of VEGF *in vitro*. It has been speculated that VEGF and SDF-1 may synergistically induce tumor angiogenesis [50]. Through the upregulation of CXCR4 on vascular endothelial cells, VEGF synergizes SDF-1–mediated vascular endothelial cell migration and expansion. Carr et al. [51] have demonstrated in the *in vitro* aortic ring model that despite the absence of

circulating endothelial precursor cells, exogenous SDF-1 increases vascular sprouting. In parallel, Orimo et al. [39] have shown with an indirect experimental approach that carcinoma-associated fibroblasts, which secrete great amounts of SDF-1, promote angiogenesis by recruiting endothelial precursor cells. In these experiments, the role of SDF-1 in angiogenesis was supported by the fact that inhibition of the CXC chemokine significantly reduced angiogenic response [39]. These results are in contrast to those reported by Phillips et al. [33], who have demonstrated that blockade of SDF-1 did not influence the process of tumor vascularization. In the present study, we demonstrate in a direct experimental approach that exogenous application of SDF-1 indeed affects the angiogenesis and vascularization of colorectal tumors *in vivo*. However, SDF-1 did not induce an overall increase in the number of newly formed blood vessels, but specifically accelerated the process of blood vessel formation. This action most probably involved an increase in VEGF expression because SDF-1–treated tumors showed a significant dilation of their blood vessels compared to those of PBS-treated controls, which may be caused by the well-known dilatory action of the growth factor.

In conclusion, we have demonstrated that the chemokine SDF-1 promotes solid metastatic tumor growth by proproliferative and antiapoptotic actions in an angiogenesis-dependent manner. Our results therefore indicate that the SDF-1/CXCR4 signaling pathway may be a promising target for adjuvant antitumor therapy.

Acknowledgements

We appreciate the technical assistance of C. Marx, J. Becker, and R. M. Nickels.

References

[1] Abdalla EK, Vauthey JN, Ellis LM, Ellis V, Pollock R, Broglio KR, Hess K, and Curley SA (2004). Recurrence and outcomes following hepatic resection, radiofrequency ablation, and combined resection/ablation for colorectal liver metastases. *Ann Surg* **239**, 818–825.

[2] Choti MA, Sitzmann JV, Tiburi MF, Sumetchotimetha W, Rangsin R, Schulick RD, Lillemoe KD, Yeo CJ, and Cameron JL (2002). Trends in long-term survival following liver resection for hepatic colorectal metastases. *Ann Surg* **235**, 759–766.

[3] Yamamoto J, Shimada K, Kosuge T, Yamasaki S, Sakamoto M, and Fukuda H (1999). Factors influencing survival of patients undergoing hepatectomy for colorectal metastases. *Br J Surg* **86**, 332–337.

[4] Fong Y (1999). Surgical therapy of hepatic colorectal metastasis. *CA Cancer J Clin* **49**, 231–255.

[5] Elias D, Liberale G, Vernerey D, Pocard M, Ducreux M, Boige V, Malka D, Pignon JP, and Lasser P (2005). Hepatic and extrahepatic colorectal metastases: when resectable, their localization does not matter, but their total number has a prognostic effect. *Ann Surg Oncol* **12**, 900–909.

[6] Labow DM, Buell JE, Yoshida A, Rosen S, and Posner MC (2002). Isolated pulmonary recurrence after resection of colorectal hepatic metastases—is resection indicated? *Cancer J* **8**, 342–347.

[7] Yoshidome H, Ito H, Kimura F, Ambiru S, Shimizu H, Togawa A, Ohtsuka M, Kato A, Nukui Y, and Miyazaki M (2004). Surgical treatment for extrahepatic recurrence after hepatectomy for colorectal metastases. *Hepatogastroenterology* **51**, 1805–1809.

[8] Folkman J (1992). The role of angiogenesis in tumor growth. *Semin Cancer Biol* **3**, 65–71.

[9] Chambers AF, Groom AC, and MacDonald IC (2002). Dissemination and growth of cancer cells in metastatic sites. *Nat Rev Cancer* **2**, 563–572.

[10] Baggiolini M (1998). Chemokines and leukocyte traffic. *Nature* **392**, 565–568.

[11] Burger JA and Kipps TJ (2006). CXCR4: a key receptor in the crosstalk between tumor cells and their microenvironment. *Blood* **107**, 1761–1767.

[12] Müller A, Homey B, Soto H, Ge N, Catron D, Buchanan ME, McClanahan T, Murphy E, Yuan W, Wagner SN, et al. (2001). Involvement of chemokine receptors in breast cancer metastasis. *Nature* **410**, 50–56.

[13] Guleng B, Tateishi K, Ohta M, Kanai F, Jazag A, Ijichi H, Tanaka Y, Washida M, Morikane K, Fukushima Y, et al. (2005). Blockade of the stromal cell–derived factor-1/CXCR4 axis attenuates *in vivo* tumor growth by inhibiting angiogenesis in a vascular endothelial growth factor–independent manner. *Cancer Res* **65**, 5864–5871.

[14] Zeelenberg IS, Ruuls-Van Stalle L, and Roos E (2003). The chemokine receptor CXCR4 is required for outgrowth of colon carcinoma micrometastases. *Cancer Res* **63**, 3833–3839.

[15] Ottaiano A, Franco R, Aiello Talamanca A, Liguori G, Tatangelo F, Delrio P, Nasti G, Barletta E, Facchini G, Daniele B, et al. (2006). Overexpression of both CXC chemokine receptor 4 and vascular endothelial growth factor proteins predicts early distant relapse in stage II–III colorectal cancer patients. *Clin Cancer Res* **12**, 2795–2803.

[16] Kim J, Mori T, Chen SL, Amersi FF, Martinez SR, Kuo C, Turner RR, Ye X, Bilchik AJ, Morton DL, et al. (2006). Chemokine receptor CXCR4 expression in patients with melanoma and colorectal cancer liver metastases and the association with disease outcome. *Ann Surg* **244**, 113–120.

[17] Kollmar O, Schilling MK, and Menger MD (2004). Experimental liver metastasis: standards for local cell implantation to study isolated tumor growth in mice. *Clin Exp Metastasis* **21**, 453–460.

[18] Menger MD and Lehr HA (1993). Scope and perspectives of intravital microscopy—bridge over from *in vitro* to *in vivo*. *Immunol Today* **14**, 519–522.

[19] Lehr HA, Leunig M, Menger MD, Nolte D, and Messmer K (1993). Dorsal skinfold chamber technique for intravital microscopy in nude mice. *Am J Pathol* **143**, 1055–1062.

[20] Menger MD, Laschke MW, and Vollmar B (2002). Viewing the microcirculation through the window: some twenty years experience with the hamster dorsal skinfold chamber. *Eur Surg Res* **34**, 83–91.

[21] Vajkoczy P, Farhadi M, Gaumann A, Heidenreich R, Erber R, Wunder A, Tonn JC, Menger MD, and Breier G (2002). Microtumor growth initiates angiogenic sprouting with simultaneous expression of VEGF, VEGF receptor-2, and angiopoietin-2. *J Clin Invest* **109**, 777–785.

[22] Rupertus K, Kollmar O, Scheuer C, Junker B, Menger MD, and Schilling MK (2007). Major but not minor hepatectomy accelerates engraftment of extrahepatic tumor cells. *Clin Exp Metastasis* **24**, 39–48.

[23] Erber R, Thurnher A, Katsen AD, Groth G, Kerger H, Hammes HP, Menger MD, Ullrich A, and Vajkoczy P (2004). Combined inhibition of VEGF and PDGF signaling enforces tumor vessel regression by interfering with pericyte-mediated endothelial cell survival mechanisms. *FASEB J* **18**, 338–340.

[24] Kollmar O, Junker B, Rupertus K, Menger MD, and Schilling MK (2007). Studies on MIP-2 and CXCR2 expression in a mouse model of extrahepatic colorectal metastasis. *Eur J Surg Oncol* **33**, 803–811.

[25] Kollmar O, Junker B, Rupertus K, Scheuer C, Menger MD, and Schilling MK (2007). Liver resection–associated macrophage inflammatory protein-2 stimulates engraftment but not growth of colorectal metastasis at extrahepatic sites. *J Surg Res* (Epub 2007 June 8).

[26] Burns JM, Summers BC, Wang Y, Melikian A, Berahovich R, Miao Z, Penfold ME, Sunshine MJ, Littman DR, Kuo CJ, et al. (2006). A novel chemokine receptor for SDF-1 and I-TAC involved in cell survival, cell adhesion, and tumor development. *J Exp Med* **203**, 2201–2213.

[27] Tilton B, Ho L, Oberlin E, Loetscher P, Baleux F, Clark-Lewis I, and Thelen M (2000). Signal transduction by CXC chemokine receptor 4. Stromal cell–derived factor 1 stimulates prolonged protein kinase B and extracellular signal–regulated kinase 2 activation in T lymphocytes. *J Exp Med* **192**, 313–324.

[28] Darash-Yahana M, Pikarsky E, Abramovitch R, Zeira E, Pal B, Karplus R, Beider K, Avniel S, Kasem S, Galun E, et al. (2004). Role of high expression levels of CXCR4 in tumor growth, vascularization, and metastasis. *FASEB J* **18**, 1240–1242.

[29] Engl T, Relja B, Marian D, Blumenberg C, Muller I, Beecken WD, Jones J, Ringel EM, Bereiter-Hahn J, Jonas D, et al. (2006). CXCR4 chemokine receptor mediates prostate tumor cell adhesion through alpha5 and beta3 integrins. *Neoplasia* **8**, 290–301.

[30] Strieter RM, Belperio JA, Phillips RJ, and Keane MP (2004). CXC chemokines in angiogenesis of cancer. *Semin Cancer Biol* **14**, 195–200.

[31] Balkwill F (2003). Chemokine biology in cancer. *Semin Immunol* **15**, 49–55.

[32] Loberg RD, Day LL, Harwood J, Ying C, St John LN, Giles R, Neeley CK, and Pienta KJ (2006). CCL2 is a potent regulator of prostate cancer cell migration and proliferation. *Neoplasia* **8**, 578–586.
[33] Phillips RJ, Burdick MD, Lutz M, Belperio JA, Keane MP, and Strieter RM (2003). The stromal derived factor-1/CXCL12–CXC chemokine receptor 4 biological axis in non–small cell lung cancer metastases. *Am J Respir Crit Care Med* **167**, 1676–1686.
[34] Ohira S, Sasaki M, Harada K, Sato Y, Zen Y, Isse K, Kozaka K, Ishikawa A, Oda K, Nimura Y, et al. (2006). Possible regulation of migration of intrahepatic cholangiocarcinoma cells by interaction of CXCR4 expressed in carcinoma cells with tumor necrosis factor-alpha and stromal-derived factor-1 released in stroma. *Am J Pathol* **168**, 1155–1168.
[35] Brand S, Dambacher J, Beigel F, Olszak T, Diebold J, Otte JM, Goke B, and Eichhorst ST (2005). CXCR4 and CXCL12 are inversely expressed in colorectal cancer cells and modulate cancer cell migration, invasion and MMP-9 activation. *Exp Cell Res* **310**, 117–130.
[36] Ottaiano A, di Palma A, Napolitano M, Pisano C, Pignata S, Tatangelo F, Botti G, Acquaviva AM, Castello G, Ascierto PA, et al. (2005). Inhibitory effects of anti-CXCR4 antibodies on human colon cancer cells. *Cancer Immunol Immunother* **54**, 781–791.
[37] Pan J, Mestas J, Burdick MD, Phillips RJ, Thomas GV, Reckamp K, Belperio JA, and Strieter RM (2006). Stromal derived factor-1 (SDF-1/CXCL12) and CXCR4 in renal cell carcinoma metastasis. *Mol Cancer* **5**, 56.
[38] Zhang L, Yeger H, Das B, Irwin MS, and Baruchel S (2007). Tissue microenvironment modulates CXCR4 expression and tumor metastasis in neuroblastoma. *Neoplasia* **9**, 36–46.
[39] Orimo A, Gupta PB, Sgroi DC, Arenzana-Seisdedos F, Delaunay T, Naeem R, Carey VJ, Richardson AL, and Weinberg RA (2005). Stromal fibroblasts present in invasive human breast carcinomas promote tumor growth and angiogenesis through elevated SDF-1/CXCL12 secretion. *Cell* **121**, 335–348.
[40] Barbero S, Bonavia R, Bajetto A, Porcile C, Pirani P, Ravetti JL, Zona GL, Spaziante R, Florio T, and Schettini G (2003). Stromal cell–derived factor 1alpha stimulates human glioblastoma cell growth through the activation of both extracellular signal–regulated kinases 1/2 and Akt. *Cancer Res* **63**, 1969–1974.
[41] Lee BC, Lee TH, Avraham S, and Avraham HK (2004). Involvement of the chemokine receptor CXCR4 and its ligand stromal cell–derived factor 1alpha in breast cancer cell migration through human brain microvascular endothelial cells. *Mol Cancer Res* **2**, 327–338.
[42] Datta SR, Dudek H, Tao X, Masters S, Fu H, Gotoh Y, and Greenberg ME (1997). Akt phosphorylation of BAD couples survival signals to the cell-intrinsic death machinery. *Cell* **91**, 231–241.
[43] Cardone MH, Roy N, Stennicke HR, Salvesen GS, Franke TF, Stanbridge E, Frisch S, and Reed JC (1998). Regulation of cell death protease caspase-9 by phosphorylation. *Science* **282**, 1318–1321.
[44] Kops GJ, de Ruiter ND, De Vries-Smits AM, Powell DR, Bos JL, and Burgering BM (1999). Direct control of the Forkhead transcription factor AFX by protein kinase B. *Nature* **398**, 630–634.
[45] Strieter RM, Polverini PJ, Kunkel SL, Arenberg DA, Burdick MD, Kasper J, Dzuiba J, Van Damme J, Walz A, Marriott D, et al. (1995). The functional role of the ELR motif in CXC chemokine-mediated angiogenesis. *J Biol Chem* **270**, 27348–27357.
[46] Bachelder RE, Wendt MA, and Mercurio AM (2002). Vascular endothelial growth factor promotes breast carcinoma invasion in an autocrine manner by regulating the chemokine receptor CXCR4. *Cancer Res* **62**, 7203–7206.
[47] Salcedo R and Oppenheim JJ (2003). Role of chemokines in angiogenesis: CXCL12/SDF-1 and CXCR4 interaction, a key regulator of endothelial cell responses. *Microcirculation* **10**, 359–370.
[48] Tachibana K, Hirota S, Iizasa H, Yoshida H, Kawabata K, Kataoka Y, Kitamura Y, Matsushima K, Yoshida N, Nishikawa S, et al. (1998). The chemokine receptor CXCR4 is essential for vascularization of the gastrointestinal tract. *Nature* **393**, 591–594.
[49] Yang SX, Chen JH, Jiang XF, Wang QL, Chen ZQ, Zhao W, Feng YH, Xin R, Shi JQ, and Bian XW (2005). Activation of chemokine receptor CXCR4 in malignant glioma cells promotes the production of vascular endothelial growth factor. *Biochem Biophys Res Commun* **335**, 523–528.
[50] Kryczek I, Lange A, Mottram P, Alvarez X, Cheng P, Hogan M, Moons L, Wei S, Zou L, Machelon V, et al. (2005). CXCL12 and vascular endothelial growth factor synergistically induce neoangiogenesis in human ovarian cancers. *Cancer Res* **65**, 465–472.
[51] Carr AN, Howard BW, Yang HT, Eby-Wilkens E, Loos P, Varbanov A, Qu A, DeMuth JP, Davis MG, Proia A, et al. (2006). Efficacy of systemic administration of SDF-1 in a model of vascular insufficiency: support for an endothelium-dependent mechanism. *Cardiovasc Res* **69**, 925–935.